Article

Cell Reports

c-Abl Regulates Proteasome Abundance by Controlling the Ubiquitin-Proteasomal Degradation of PSMA7 Subunit

Graphical Abstract

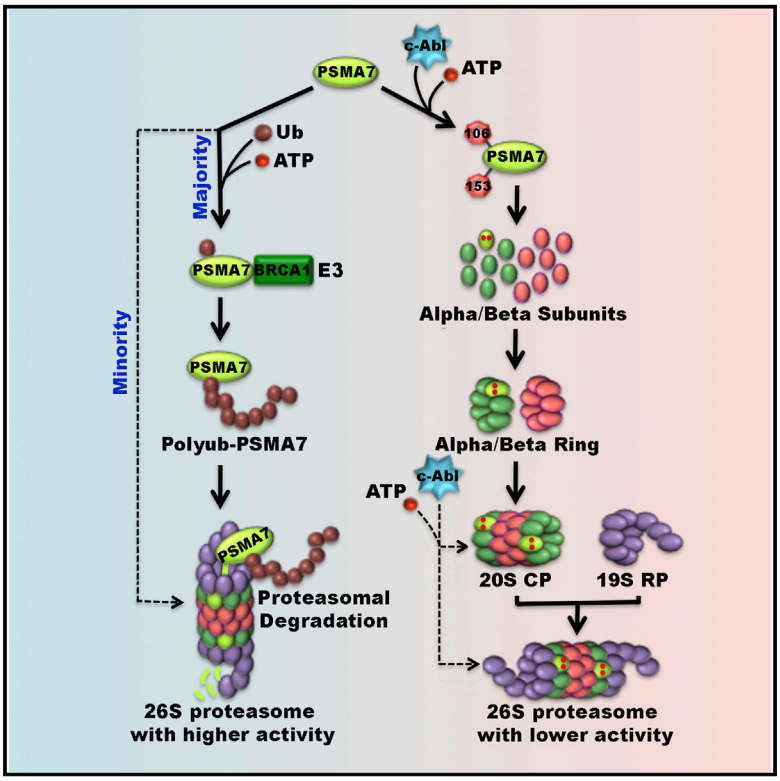

Highlights

- The 20S proteasome subunit PSMA7 is subjected to ubiquitin-proteasomal degradation
- PSMA7 degradation is suppressed by c-Abl-mediated tyrosine phosphorylation at Y106
- Proteasome abundance is decreased by *c-abl/arg* knockout or Abl kinase inhibition
- c-Abl plays dual roles in the regulation of proteasome homeostasis and activities

Authors

Dapei Li, Qincai Dong, ..., Xuan Liu, Cheng Cao

Correspondence

liux931932@163.com (X.L.), caoc@nic.bmi.ac.cn (C.C.)

In Brief

Proteasome is responsible for cellular protein proteolysis, but the turnover of the proteasome subunit itself is still unknown. Li et al. show that the ubiquitin-proteasomal degradation of PSMA7 subunit and cellular proteasome abundance is regulated by c-Abl kinase. c-Abl plays dual roles in the regulation of proteasome homeostasis and activities.

Li et al., 2015, Cell Reports *10*, 484–496
February 3, 2015
http://dx.doi.org/10.1016/j.celrep.2014.12.044

OPEN ACCESS
CellPress

Cell Reports
Article

c-Abl Regulates Proteasome Abundance by Controlling the Ubiquitin-Proteasomal Degradation of PSMA7 Subunit

Dapei Li,[1] Qincai Dong,[1] Qingping Tao,[4] Jing Gu,[1] Yan Cui,[1] Xuefeng Jiang,[1] Jing Yuan,[2] Weihua Li,[3] Rao Xu,[1] Yanwen Jin,[1] Ping Li,[1] David T. Weaver,[4] Qingjun Ma,[1] Xuan Liu,[1,*] and Cheng Cao[1,*]
[1]Beijing Institute of Biotechnology, Beijing 100850, China
[2]Beijing Institute of Disease Control and Prevention, Beijing 100071, China
[3]National Center of Biomedical Analysis, Beijing 100850, China
[4]Institute of Health Sciences, Anhui University, Hefei 230601, China
*Correspondence: liux931932@163.com (X.L.), caoc@nic.bmi.ac.cn (C.C.)
http://dx.doi.org/10.1016/j.celrep.2014.12.044

SUMMARY

The ubiquitin-proteasome system is a vital proteolytic pathway required for cell homeostasis. However, the turnover mechanism of the proteasome subunit itself is still not understood. Here, we show that the 20S proteasome subunit PSMA7 is subjected to ubiquitination and proteasomal degradation, which was suppressed by PSMA7 phosphorylation at Y106 mediated by the nonreceptor tyrosine kinases c-Abl/Arg. BRCA1 specifically functions as an E3 ubiquitin ligase of PSMA7 ubiquitination. c-Abl/Arg regulates cellular proteasome abundance by controlling the PSMA7 subunit supply. Downregulated PSMA7 level results in decreased proteasome abundance in c-Abl/Arg RNAi-knockdown or *c-abl/arg*-deficient cells, which demonstrated an increased sensitivity to proteasome inhibition. In response to oxidative stress, the c-Abl-mediated upregulation of proteasome level compensates for the proteasomal activity impairment induced by reactive oxygen species. Abl-kinases-regulated biogenesis and homeostasis of proteasome complexes may be important for understanding related diseases and pathological states.

INTRODUCTION

ATP-dependent ubiquitin-proteasomal proteolysis is responsible for rapid and irreversible protein turnover in the cell (Finley, 2009; Pickart and Cohen, 2004). In mammals, the evolutionarily conserved proteasome contains at least 33 different protein subunits (Bedford et al., 2010; Murata et al., 2009). The 20S core particle (CP) of the proteasome is arranged into four-stacked hetero-oligomeric rings ($\alpha\beta\beta\alpha$) composed of seven α subunits ($\alpha1$–$\alpha7$) and seven β subunits ($\beta1$–$\beta7$), three of which ($\beta1$, $\beta2$, and $\beta5$) are proteolytically active subunits (Groll et al., 1997). The 20S CP is usually capped at one or both ends by the 19S regulatory particle to form a complete 26S/30S proteasome (Leggett et al., 2002; Navon and Goldberg, 2001).

The biogenesis of the proteasome is a highly orchestrated, multistep event involving the biosynthesis, assembly, and maturation of each of the subunits. Coordinated transcription of proteasome subunit (PSM) genes is regulated by nuclear-factor-erythroid-derived 2-related factor 1 (Nrf1) and Nrf2 in mammals (Pickering et al., 2012; Radhakrishnan et al., 2010) and by the short-lived transcription factor Rpn4 in yeast (Xie and Varshavsky, 2001). The maturation of mammalian 20S proteasome is significantly dependent on proteasome assembling chaperones and proteassemblin POMP (Le Tallec et al., 2007; Murata et al., 2009). Proteasome abundance is also highly regulated by proteasome turnover, which contributes to a rapid switch between constitutive proteasome and immunoproteasome in response to interferon-γ (Heink et al., 2005). However, to our knowledge, the mechanism by which the turnover of constitutive 20S CP subunits is regulated is still unknown.

The nonreceptor tyrosine kinases c-Abl (Abl1) and Arg (*abl*-related gene; Abl2) are ubiquitously expressed in mammalian tissues and share ~90% homology at N-terminal SH3, SH2, and kinase domain, implying their overlapping functions related to cell proliferation, survival, adhesion, migration, and cellular stress responses (Pendergast, 2002). c-Abl is activated by stimuli such as growth factors, reactive oxygen species (ROS), and DNA damages (Plattner et al., 1999; Sun et al., 2000). Mice with disruption of c-Abl or Arg are viable, whereas embryos deficient in both *c-abl* and *arg* exhibit defects in neurulation and die prior to 11 days postcoitus, which suggests that c-Abl/Arg may play pivotal functions in developmental processes (Koleske et al., 1998). Notably, as a result of chromosomal translocation, the constitutively active Bcr-Abl chimeric proteins that present in 95% of patients with chronic myeloid leukemia (CML) were shown to be involved in CML by inducing abnormal cell proliferation, adhesion, migration, and DNA repair pathways.

The PSMA7 ($\alpha4$) subunit is one of the constitutive α subunits of mammalian 20S proteasome and an association target of specific proteasome-regulation proteins (Cho et al., 2001; Dächsel et al., 2005). Our previous work has shown that the c-Abl and Arg tyrosine kinases directly interact with and phosphorylate

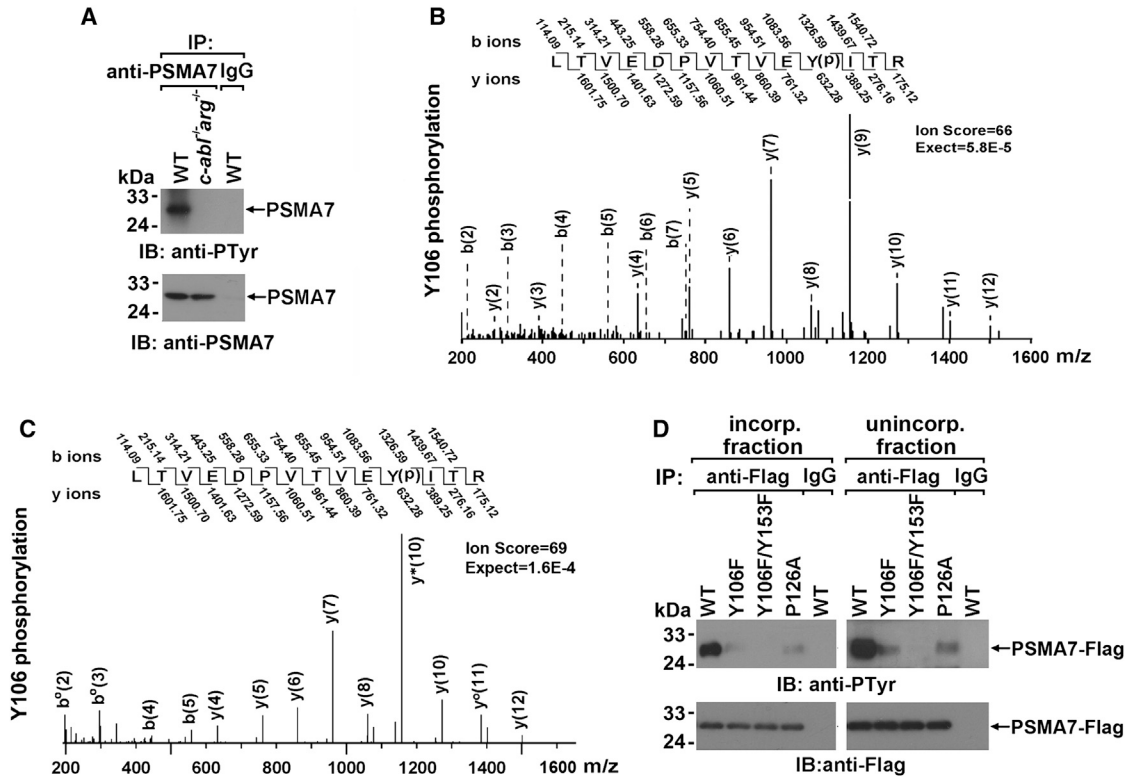

Figure 1. c-Abl Kinase Phosphorylates PSMA7 at Y106

(A) Anti-PSMA7 immunoprecipitates prepared from the whole lysates of wild-type or *c-abl*$^{-/-}$*arg*$^{-/-}$ MEFs were normalized by PSMA7 level and then analyzed by immunoblotting. IgG immunoprecipitates were used as a control. IB, immunoblot; IP, immunoprecipitation; WT, wild-type.

(B and C) PSMA7-FLAG coexpressed with Myc-c-Abl in the whole (B) or fractionated proteasome-containing fraction (C) of HEK293 cells extracts were purified by anti-FLAG immunoprecipitation and then subjected to trypsinization and LC-MS/MS analysis. The monophosphorylated peptides ^{96}LTVEDPVTVEY(P)ITR^{109} containing PO_3^--modified Y106 were identified.

(D) Anti-FLAG immunoprecipitates prepared from the fractionated lysates of HEK293 cells coexpressing Myc-c-Abl and the indicated proteins were normalized by PSMA7-FLAG level and then detected by immunoblotting.

the PSMA7 subunit both in vitro and in vivo and that proteasomes loaded with tyrosine-phosphorylated PSMA7 have decreased proteolytic activity (Liu et al., 2006). In this study, we expanded on this work to show that Abl-kinases-mediated PSMA7 phosphorylation significantly suppressed the ubiquitin-proteasomal degradation of PSMA7 and therefore contributed to the regulation of cellular proteasome abundance.

RESULTS

c-Abl Kinase Phosphorylates PSMA7 at Y106

In concert with our previous findings, PSMA7 was tyrosine phosphorylated by Abl kinase in wild-type, but not in *c-abl/arg*-deficient, mouse embryonic fibroblasts (MEFs) (Figure 1A). To further analyze the potential phosphorylation site, the FLAG-tagged PSMA7 ectopically coexpressed with c-Abl in HEK293 cells was subjected to mass spectrometry analysis (liquid chromatography-tandem mass spectrometry [LC-MS/MS]). The results showed that, in addition to Y153 (Liu et al., 2006; Rush et al., 2005; Figure S1A), Y106 of PSMA7 was also phosphorylated (Figure 1B). Further, proteasome-incorporated exogenous PSMA7 was prepared by gel filtration (fraction no. 4–no. 6 with proteasomal peptidase activity; Figures S1B and S1C) followed by anti-FLAG immunoprecipitation; both Y106 and Y153 on proteasome-incorporated PSMA7 were further confirmed by LC-MS/MS (Figures 1C and S1D).

By phosphorylation-deficient mutation, it was further demonstrated that the proteasome-incorporated or unincorporated PSMA7 was similarly phosphorylated at Y106 by c-Abl kinase (Figure 1D). Moreover, PSMA7(P126A), a c-Abl-association-defective mutant due to mutation within the PXXP consensus motif essential for c-Abl SH3 binding (Ren et al., 1993; Figure S1E), also demonstrated impaired phosphorylation (Figure 1D). The significantly decreased tyrosine phosphorylation on PSMA7 with only Y106F mutation may be likely explained by the fact that many tyrosine kinases, such as Src or epidermal growth factor receptor, show synergistic effects with the activity at multiple phosphorylate sites in a substrate.

c-Abl-Mediated Phosphorylation Regulates PSMA7 Expression

It was found that the ectopically expressed PSMA7, but not other alpha subunits, was upregulated by c-Abl or Arg (Figure 2A). Moreover, the proteasome-unincorporated exogenous PSMA7

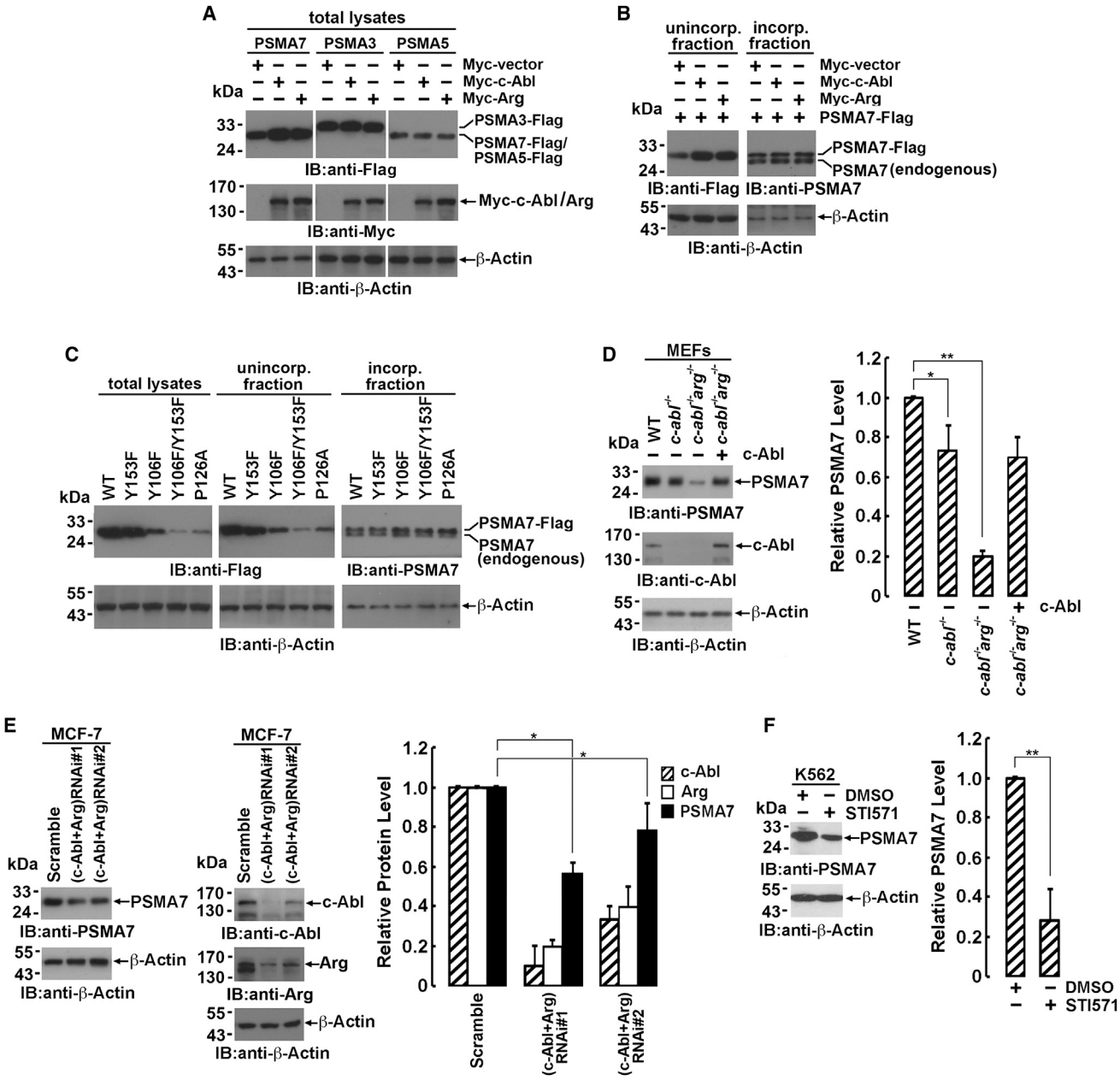

Figure 2. c-Abl-Mediated Phosphorylation Regulates PSMA7 Expression

(A–C) The exogenously expressed PSMA7 levels in the whole (A) or fractionated (B and C) lysates of HEK293 cells transfected with the indicated plasmids were detected by immunoblotting.

(D–F) The whole lysates of indicated cells were detected by immunoblotting. *c-abl*$^{-/-}$*arg*$^{-/-}$ MEFs were rescued by the electrotransfection of c-Abl-expressing plasmid (D). (c-Abl+Arg)RNAi no. 1 and no. 2 are two different c-Abl/Arg double-knockdown cell lines (E). K562 CML cells were treated with 10 μM STI571 or DMSO for 18 hr (F). The qualification of three independent experiments was presented as the mean ± SD (*$p < 0.05$; **$p < 0.005$).

(endogenous PSMA7 was hardly detected in unincorporated fractions as shown by Figure S2A) level was clearly upregulated by the coexpression of c-Abl or Arg, whereas the incorporated PSMA7 level was not much affected (Figure 2B). In concert with the findings, PSMA7 containing Y106F or P126A mutation demonstrated a more significantly decreased expression level than Y153F mutation did, in proteasome-unincorporated, but not incorporated, fraction (Figure 2C). The observation that the phosphorylation-deficient PSMA7 could be properly incorporated into proteasome suggested that the incorporation of PSMA7 was not much regulated by its tyrosine phosphorylation (Figure 2C).

Further, it was observed that, although PSMA7 level was moderately decreased in the *c-abl*$^{-/-}$ MEFs compared with

that in wild-type MEFs, it was remarkably decreased in *c-abl*$^{-/-}$*arg*$^{-/-}$ MEFs (Figure 2D), indicating the redundant function of c-Abl and Arg in PSMA7 regulation. PSMA7 expression was significantly rescued by the reintroduction of c-Abl (Figure 2D), but not kinase-dead c-Abl(K290R) (Figure S2B). Obvious PSMA7 downregulation was also observed in two independent c-Abl/Arg double-knockdown MCF-7 cell lines generated by RNAi (Figures 2E and S2C) or in c-Abl/Arg-specific inhibitor STI571-treated K562 CML cells that express constitutively active Bcr-Abl (Figure 2F). Unlike PSMA5, little if any PSMA7 was found to be present as a free monomer in tested cells by gel filtration (Figure S2A), which was in concert with the other reports (Jørgensen and Hendil, 1999). Therefore, the PSMA7 detected in the above experiments (Figures 2D–2F) primarily arose from PSMA7 in proteasome complexes. These results suggested that, in physiological contexts, c-Abl may regulate the level of proteasome-incorporated PSMA7 by modulating PSMA7 supply for proteasome assembly. However, c-Abl had little if any effect on proteasome level when PSMA7 was sufficiently supplied (Figures 2B and 2C, right panels).

c-Abl-Mediated Phosphorylation Inhibits the Ubiquitin-Proteasomal Degradation of PSMA7

Little if any effect on PSMA7 mRNA level was observed by *c-abl/arg* deficiency (Figure S3A). We next investigated the mechanism other than transcription responsible for c-Abl/Arg-regulated free PSMA7 level in detail using a N-terminal FLAG-tagged PSMA7 (FLAG-PSMA7), which was similarly regulated by c-Abl (Figures S3B and S3C) and less presented as an incorporated form than PSMA7-FLAG (~3% versus ~10%) due to the lower incorporation efficiency (Groll et al., 1997; Figure S3D). Therefore, the interference of incorporated, long-living PSMA7 could be better avoided (Figures 2C and 3C). The pulse-chase experiment by [^{35}S]-methionine labeling demonstrated that the half-life of wild-type PSMA7 was extended from ~20 hr to more than 60 hr by coexpression of c-Abl or Arg (Figure 3A). Comparing with Y153F mutant (~15 hr), the half-life of the mutant containing Y106F or P126A was significantly decreased to ~6 hr and ~9 hr, respectively. A similarly lowered stability was also observed when wild-type or Y106F mutant PSMA7 was expressed in *c-abl*$^{-/-}$*arg*$^{-/-}$ MEFs, indicating that PSMA7 stability was dependent on Abl kinases, but not due to a structural problem associated with the Y106F mutation (Figure 3B).

In concert with the findings that c-Abl regulates the expression of free other than proteasome-incorporated PSMA7 (Figures 2B and 2C), the stability of proteasome-unincorporated, but not incorporated, PSMA7 was significantly regulated by Y106 phosphorylation in cycloheximide (CHX)-treated cells (Figure 3C). Also, the proteasome complex stability was not much effected by the incorporation of ectopically expressed wild-type or Y106F PSMA7 (Figure 3C, lower panel), implying that Abl-mediated PSMA7 phosphorylation may modulate proteasome level by regulating PSMA7 supply for newborn proteasome, but not the turnover of assembled proteasomes.

Next, we found that the lowered PSMA7 levels in *c-abl*$^{-/-}$*arg*$^{-/-}$ MEFs can be partially rescued by proteasome inhibitor lactacystin, but not by lysosomal inhibitor concanamycin A (Li et al., 2010; Figure 3D). The half-life of exogenous PSMA7 was also prolonged by lactacystin treatment (Figure 3E). In vitro degradation assay also demonstrated that proteasome inhibitor MG132 could suppress the degradation of both [^{35}S]-labeled wild-type and Y106F PSMA7 in the absence of c-Abl (Figure 3F). Notably, the degradation of wild-type, but not Y106F, PSMA7 was significantly blocked after the pretreatment by recombinant c-Abl kinase. These results indicate that the PSMA7 subunit is susceptible to proteasomal degradation in the absence of the c-Abl kinase.

Further, a distinct polyubiquitination of exogenously expressed PSMA7 was observed after MG132 treatment, which was decreased by more than 70% by the coexpression of c-Abl, but not c-Abl(K290R) (Figure 3G, left panel). Consistent with the significantly decreased stability, PSMA7(Y106F), PSMA7(Y106/153F), or PSMA7(P126A) mutants each demonstrated robust polyubiquitination compared with wild-type or PSMA7(Y153F) (Figure 3G, right panel). Polyubiquitination was substantially impaired upon the expression of conjugation-deficient ubiquitin Ub(G76A) (Figure 3H).

Then, the anti-FLAG immunoprecipitates prepared from the extracts of HEK293-expressing FLAG-PSMA7(Y106F) were resolved by SDS-PAGE. Both PSMA7 and ubiquitin were found to be present in the protein bands assayed ranging from 35 to 140 kDa by LC-MS/MS analysis (Figure S3E; Table S1). Quantitative proteomics demonstrated the ubiquitin modification on K115 of PSMA7 (Kim et al., 2011). Accordingly, compared with the PSMA7(Y106F), PSMA7(Y106F/K115R) had significantly impaired polyubiquitination (Figure 3I), as well as partially rescued PSMA7 expression (Figure 3J). The polyubiquitination of FLAG-PSMA7(Y106F) was also detected by anti-FLAG immunoblotting, excluding the false-positive polyubiquitination signals of PSMA7-associated polyubiquitinated proteins (Figure 3I, right panel). These findings collectively support the hypothesis that the c-Abl kinase regulates the ubiquitination and then the proteasomal degradation of PSMA7.

The Ubiquitin-Protein Ligase BRCA1 Is Potentially Responsible for PSMA7 Polyubiquitination

The ubiquitin ligase BRCA1 that is associated with c-Abl kinase (Foray et al., 2002) was initially identified in PSMA7(Y106F) immunoprecipitates by LC-MS/MS. Further studies showed that BRCA1 was efficiently coimmunoprecipitated with PSMA7(Y106F), but not with PSMA7(Y153F) or wild-type PSMA7 unless in the presence of STI571 (Figure 4A). Moreover, full-length BRCA1 was found to directly associate with PSMA7 expressed in *E.coli* as shown by far-western blot (Figure 4B). Notably, a proportion of PSMA7(Y106F) was found to be coeluted with BRCA1 complexes in the first fraction with UV absorbance by gel filtration (Sy et al., 2009; Figure 4C, upper panel), and the association of BRCA1 with PSMA7(Y106F) in fraction no. 1 was further confirmed (Figure 4C, lower panel). These results indicate that the polyubiquitinated PSMA7 should be proteasome unassociated, because active proteasome complexes were eluted in fractions no. 4–no. 6 (Figures S1B and S2A).

The knockdown of BRCA1 expression by RNAi resulted in compromised ubiquitination (Figure 4D) and remarkably increased expression of PSMA7(Y106F) (Figure S4A). The

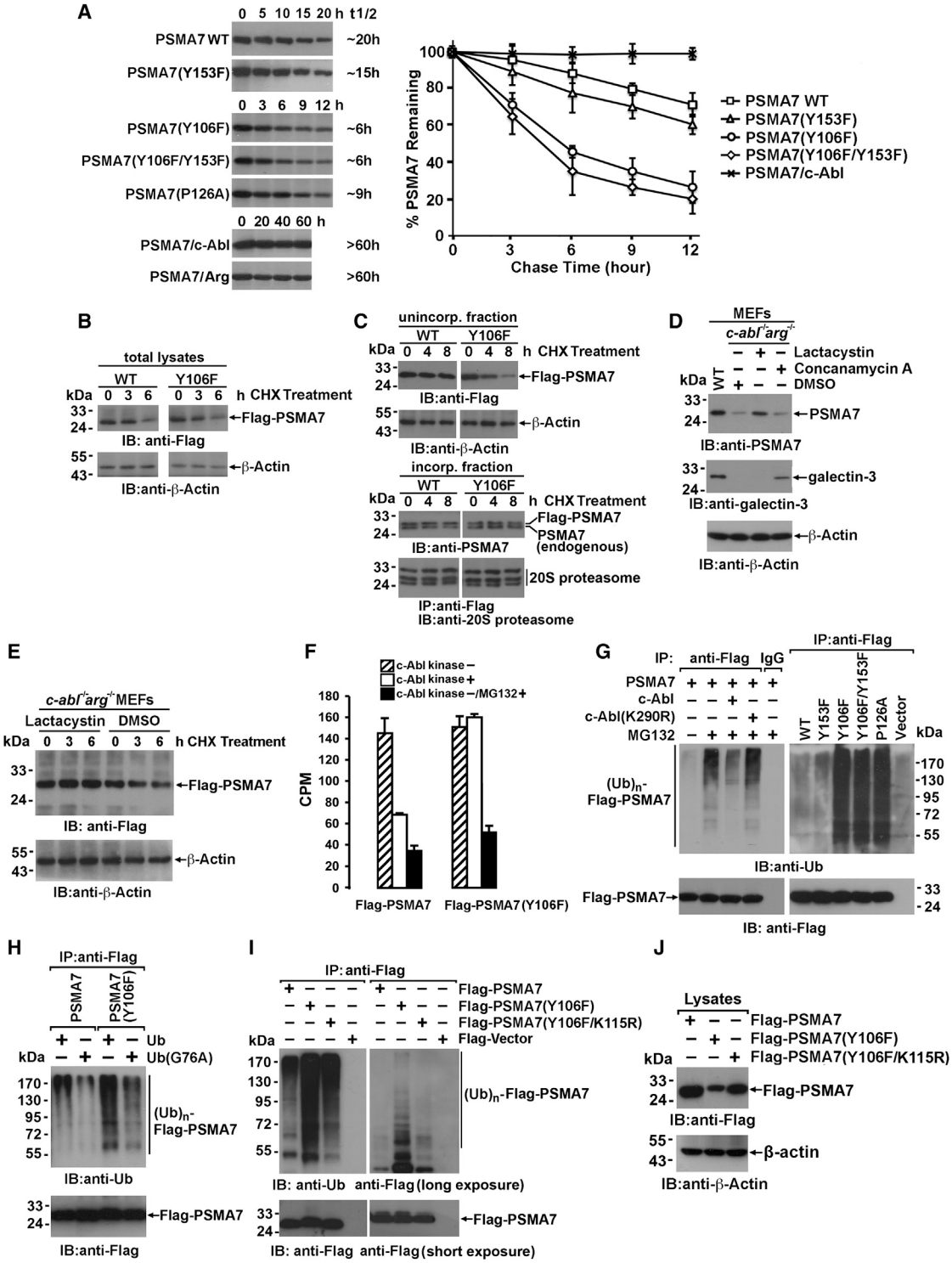

Figure 3. c-Abl-Mediated Tyrosine Phosphorylation Inhibits PSMA7 Degradation through Ubiquitin-Proteasome Pathway

(A) The indicated proteins labeled with [^{35}S]-methionine were chased for indicated time in HEK293 cells. Anti-FLAG immunoprecipitates were analyzed by SDS-PAGE electrophoresis and autoradiography. The stability (% PSMA7 remaining) was indicated as the mean ± SD of three independent experiments.

(B) The level of exogenous PSMA7 in the whole lysates of *c-abl*$^{-/-}$*arg*$^{-/-}$ MEFs treated with 100 μg/ml cycloheximide (CHX) was chased for indicated time and analyzed by immunoblotting.

(legend continued on next page)

polyubiquitination of PSMA7(Y106F) was not observed in BRCA1-deficient HCC1937 breast carcinoma cells unless an exogenously active BRCA1, but not the enzymatically inactive BRCA1(I26A), was reintroduced into the cells (Figure 4E). Similarly, significant polyubiquitination of PSMA7 was observed only if BRCA1, but not BRCA1(I26A) mutant, was added into in vitro ubiquitination system together with BARD1 (Figure 4F). In vitro polyubiquitination of PSMA7 was suppressed with the presence of recombinant c-Abl kinase (Figure 4G). These results suggest that the BRCA1 is the (probably not the only) E3 ubiquitin ligase of PSMA7 with Y106 phosphorylation deficiency. Moreover, little if any difference between the half-life, ubiquitination, and BRCA interaction of FLAG-PSMA7 and PSMA7-FLAG was observed (Figures S4B–S4D), excluding the possibility that the ubiquitination and degradation of FLAG-PSMA7 were raised by its lower incorporation efficiency.

Cellular Proteasome Abundance Is Controlled by PSMA7 Stability

We next sought to determine whether the Abl-kinases-regulated supply of PSMA7 was involved in the regulation of cellular proteasome abundance. Exogenous expression of c-Abl or Arg, but not the inactive mutant c-Abl(K290R) or Arg(K337R), resulted in an increased cellular proteasome abundance (Figure 5A). Moreover, comparing with wild-type cells, mature 20S proteasome levels in *c-abl/arg*-deficient or knockdown cells were decreased by ~75% and ~40%, respectively (Figure 5B). Cells bearing similar PSMA7 and proteasome level achieved by PSMA7 small interfering RNA (siRNA) retained a viability of 80%–95% (Figures 5B, S5A, and S5B). Notably, the reduced 20S proteasome level in *c-abl*$^{-/-}$*arg*$^{-/-}$ MEFs could be rescued by the exogenous introduction of c-Abl or PSMA7 (Figure 5B, left), suggesting that PSMA7 is the major (if not the only) proteasome subunit that is regulated by the Abl kinases. It was also noted that the level of other 20S subunits (Figure 5C), but not the constitutive 19S subunits (Figure S5C), was similarly downregulated in the *c-abl*$^{-/-}$*arg*$^{-/-}$ MEFs, implying that the 20S subunits are either coordinately assembled into proteasomes or are subjected to degradation rapidly.

Further, the treatment of both K562 cells and promyelocytic leukemia HL60 cells (expressing c-Abl, but not Bcr-Abl) with STI571 resulted in a dose-dependent reduction of mature proteasome level and the proteasome reduction was more remarkable in K562 cells than that in HL60 cells (Figure 5D). Moreover, the 20S proteasome level in the hepatic tissue of STI571-administrated mice was also markedly reduced by approximately 40%, as compared with control mice (**$p < 0.05$; Figure 5E).

Dual Roles of c-Abl Kinases in Physiological Proteasome-Dependent Proteolysis

Our previous study has demonstrated that the c-Abl-mediated phosphorylation of PSMA7 resulted in an inhibited proteasomal activity in vitro and in the cells (Liu et al., 2006). However, the phosphorylation of PSMA7 also contributes to the maintenance of proteasome abundance by protecting proteasome subunits from degradation. In concert with these findings, despite the proteasome level in *c-abl*$^{-/-}$*arg*$^{-/-}$ MEFs was only less than 25% of that in wild-type MEFs (the left of Figures 5B, 6A, and 6B), the *c-abl*$^{-/-}$*arg*$^{-/-}$ MEFs demonstrated only a mildly impaired overall proteasomal degradation capacity (achieved by the normalization of cellular β-actin level) by in-gel peptidase analysis (the middle of Figure 6A and the right of Figure 6B) or lysates peptidase assay (Figure S6A) with Suc-Leu-Leu-Val-Tyr-7-amino-4-methylcoumarin (LLVY-AMC) as small molecular substrates. The contradiction between cellular proteasome level and overall proteasomal degradation capacity was delineated by the observation that the proteasomal activity of a given number of proteasomes (achieved by the normalization of cellular proteasome level) in *c-abl*$^{-/-}$*arg*$^{-/-}$ MEFs was more than three times higher than that of wild-type MEFs because of *c-abl/arg* deficiency (the right of Figures 6A and 6B), which was consistent with the finding of Abl-kinase-mediated proteasome inhibition.

To investigate the proteasomal degradation of ubiquitin-conjugated substrates in living cells, wild-type and *c-abl*$^{-/-}$*arg*$^{-/-}$ MEFs were transfected with a short-lived ubiquitin-dependent proteolysis substrate, Ub-R-GFP, or a stable control, Ub-M-GFP (Dantuma et al., 2000). Ub-R-GFP has a longer half-life in the *c-abl/arg*-knockout cells than that in wild-type cells (~100 min versus ~70 min), which indicated a somewhat decelerated degradation of ubiquitinylated proteins in *c-abl/arg*-deficient cells (Figure 6C). It was also observed that more than 85% of the Ub-R-GFP could be degraded in both cell lines, whereas accordingly more Ub-R-GFP accumulation (13.6% versus 9.6% relative to Ub-M-GFP in the presence of MG132) was observed in *c-abl*$^{-/-}$*arg*$^{-/-}$ MEFs (Figure 6D), suggesting that the less-efficient degradation activity may be enough for *c-abl/arg*-deficient cells to deal with most of physiologically produced ubiquitinated proteins and maintain the viability. Notably, *c-abl*$^{-/-}$*arg*$^{-/-}$ MEFs demonstrated a much-higher sensitivity to proteasome inhibition because of the much-higher proteasomal

(C) FLAG-PSMA7 (1 μg)- or FLAG-PSMA7(Y106F) (5 μg)-transfected HEK293 cells were treated with CHX for the indicated times and then the fractionated cell lysates were analyzed by immunoblotting. To analyze the 20S proteasome bearing exogenous PSMA7, anti-FLAG immunoprecipitates prepared from the incorporated fraction were detected by immunoblotting with anti-20S proteasome antibody (the lowest panel).
(D) PSMA7 level in *c-abl*$^{-/-}$*arg*$^{-/-}$ MEFs treated with or without 10 μM lactacystin or concanamycin A (ConA) for 12 hr was analyzed by immunoblotting. Galectin-3 was used as a control that was sensitive to ConA treatment.
(E) *c-abl*$^{-/-}$*arg*$^{-/-}$ MEFs electrotransfected with FLAG-PSMA7 were pretreated with lactacystin or DMSO for 12 hr and then treated with CHX for the indicated times. The lysates were analyzed by immunoblotting.
(F) [^{35}S]-labeled FLAG-PSMA7 or FLAG-PSMA7 (Y106F) were preincubated with (open bar) or without (hatched bar) recombinant c-Abl kinase for 30 min and were then added to the extracts of *c-abl*$^{-/-}$*arg*$^{-/-}$ MEFs. The same cell extracts pretreated with 10 μM MG132 (black bar) were used as a control. The radioactivity of acid-soluble fraction was quantified by liquid scintillation counting. The results were expressed as the mean ± SD of three independent experiments.
(G–I) HEK293 cells transfected with the indicated plasmids were treated with 10 μM MG132 for 10 hr. Anti-FLAG immunoprecipitates prepared from the whole lysates of HEK293 cells were normalized by FLAG-PSMA7 level and then analyzed by immunoblotting.
(J) Lysates of HEK293 cells expressing the indicated proteins were analyzed by immunoblotting.

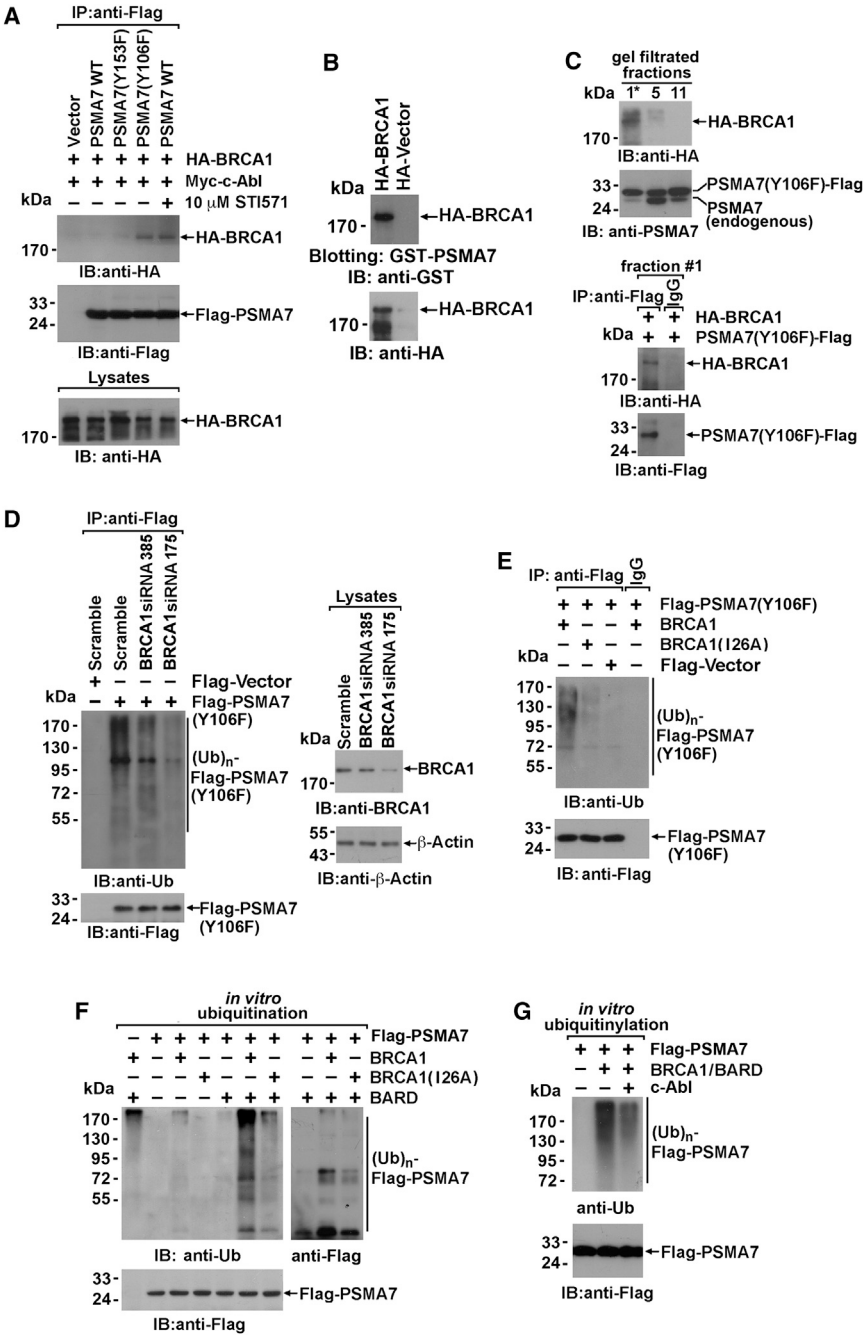

Figure 4. BRCA1 Is a Potential Ubiquitin Ligase of PSMA7

(A) Anti-FLAG immunoprecipitates prepared from the whole lysates of HEK293 cells cotransfected with indicated plasmids were normalized by FLAG-PSMA7 level and then analyzed by immunoblotting.

(B) Anti-HA immunoprecipitates prepared from cells transfected with HA-BRCA1 or HA vector were subjected to SDS-PAGE and blotted onto nitrocellulose membrane. The nitrocellulose membrane was incubated with soluble GST-PSMA7 and then analyzed by anti-GST antibody.

(C) The whole lysates of HEK293 cells coexpressing HA-BRCA1, Myc-c-Abl, and PSMA7 (Y106F)-FLAG were subjected to gel filtration. The indicated fractions (upper panel) and the anti-FLAG immunoprecipitates prepared from fraction no. 1 (lower panel) were analyzed by immunoblotting.

(D and E) Anti-FLAG immunoprecipitates or lysates prepared from MG132-treated MCF-7/scramble and MCF-7/BRCA1 siRNA cells (D) or HCC1937 cells (E) transfected with indicated plasmid were normalized by FLAG-PSMA7 level and then analyzed by immunoblotting.

(F and G) The products of the in vitro ubiquitination reactions were analyzed by immunoblotting with indicated antibodies.

activity of a given number of proteasomes but lower proteasome abundance by *c-abl/arg* deficiency (Figure 6D). Accordingly, more polyubiquitin-protein accumulation was observed by *c-abl/arg* deficiency (Figures 7G and S6B), which became more significant by MG132 treatment (the right of Figure S6B), suggesting that the *c-abl/arg*-deficient MEFs could still efficiently process the ubiquitinated proteins by partly impaired proteasomal degradation capacity.

To further address the dynamic, dual role of c-Abl and Arg in cellular proteasome-dependent proteolysis, proteasomal activity normalized to cell number was determined at different time points following the reintroduction of exogenous c-Abl or vector control into *c-abl*$^{-/-}$*arg*$^{-/-}$ MEFs. Consistent with the above findings, the PSMA7 and proteasome levels increased significantly with the expression of c-Abl (Figure 6E). Comparing with the control transfected cells, the proteasomal activity (normalized by cellular proteasome level) was sharply decreased because of the phosphorylation-mediated inhibition by gradually expressed exogenous c-Abl kinase during the initial 10 hr and was accompanied by a decreased overall cellular proteasomal degradation capacity (normalized by cellular β-actin level; Figures 6E and 6F). However, prolonged c-Abl expression resulted in a significant increase in proteasome level from 10 hr to 30 hr accompanied with the gradual recovery of overall proteasomal degradation capacity (Figures 6E and 6F).

The cytoplasmic c-Abl is activated by oxidative stress (Cao et al., 2003; Sun et al., 2000). In accordance with PSMA7 phosphorylation, the levels of both the PSMA7 subunit and proteasome complexes increased when MCF-7(Scramble), but not the c-Abl/Arg knockdown MCF-7(KD), cells were exposed to H_2O_2 (Figures 7A and 7B). The increased transcription of PSMA7 gene was not observed under toxic oxidative conditions (e.g., 0.5∼2 mM H_2O_2) that activated Abl kinase (Ding et al.,

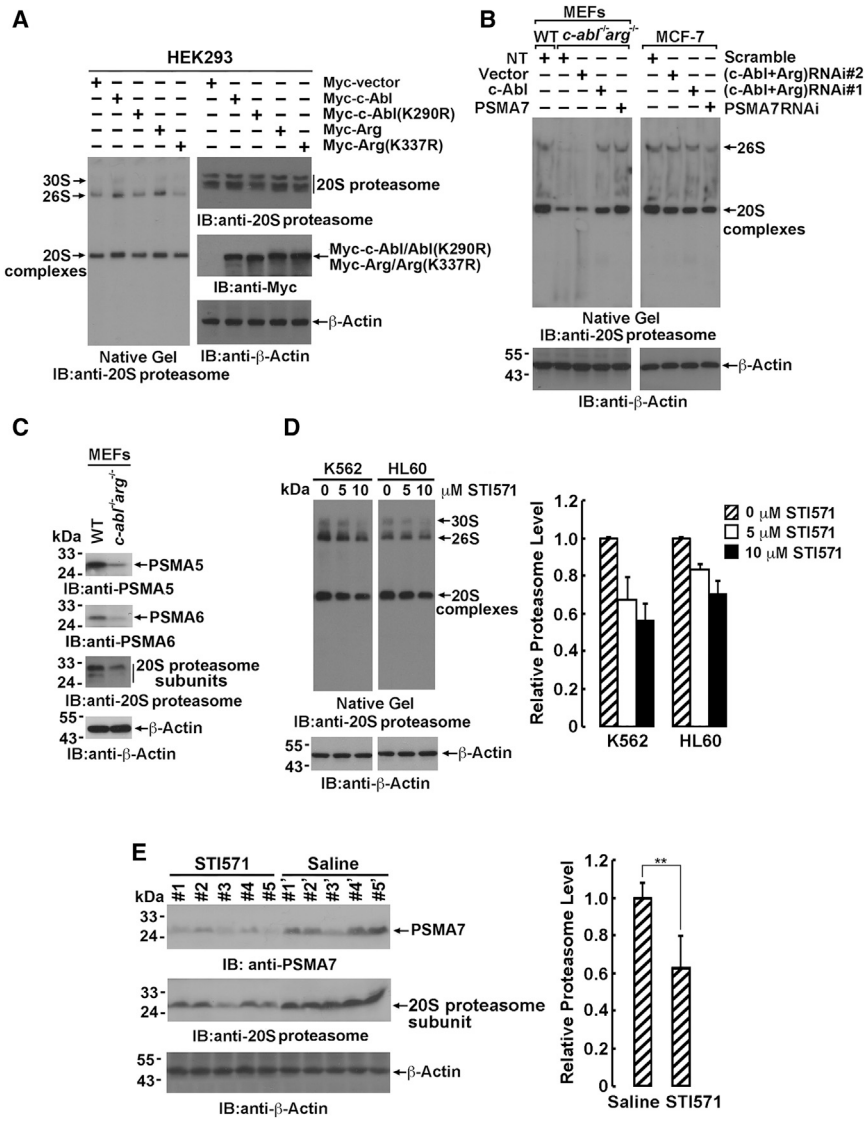

Figure 5. Proteasome Level Is Regulated by c-Abl Tyrosine Kinase

(A–D) Extracts of the indicated cells were subjected to native gel electrophoresis for proteasome complex resolution (A, B, and D) or SDS-PAGE (C) and then analyzed by immunoblotting. The qualification of three independent experiments was presented as the mean ± SD (D). NT, no treatment.

(E) Proteasome levels in hepatic cells of mice administrated with STI571 (50 mg/kg) or saline for 2 weeks were determined by immunoblotting. The difference in the relative proteasome level between the two groups was statistically significant (**$p < 0.05$).

2003; Pickering et al., 2012; Figure S7A). Similar with c-Abl/Arg knockout (Figures 6A and 6B), c-Abl/Arg knockdown resulted in a notable decrease in proteasome level (Figures 5B and 7C; 0 mM H_2O_2) but only a slight decrease in overall proteasomal degradation capacity (normalized by β-actin level; Figures 7C; 0 mM H_2O_2). The overall proteasomal degradation capacity of MCF-7(KD) cells was significantly impaired with increased H_2O_2 concentration, which was potentially due to ROS-induced inactivation of the proteasome (Aiken et al., 2011; Grune et al., 2011; Reinheckel et al., 1998). However, H_2O_2-induced impairment of overall proteasomal degradation capacity was not observed in MCF-7(Scr) cells (Figure 7C). As shown in Figure 7D, although the proteasomal activity (normalized by cellular proteasome level) in MCF-7(Scr) cells decreased according to MCF-7(KD) cells under ROS stimulus, H_2O_2-induced increase of proteasome abundance in the MCF-7(Scr) cells, but not in MCF-7(KD) cells (Figure 7C), compensated for the loss of proteasomal activity due to ROS damages. A similar result was also obtained when cells were treated with menadione, a ROS-inducing agent via redox cycling that was used as a source of vitamin K (Figures 7E and 7F). Further, comparing with wild-type cells, the polyubiquitin proteins accumulation in c-Abl/Arg knockout or knockdown cells became more accentuate when cells were exposed to ROS (Figures 7G and S7B). These results collectively support the conclusion that proteasome abundance and consequently overall proteasomal degradation capacity of the cell are dynamically regulated by c-Abl kinase activity in response to stress stimuli.

DISCUSSION

The biogenesis and proteolytic activity of 26S/30S proteasome have been comprehensively studied by the findings of functional proteasome regulator (Lee et al., 2010; Lehmann et al., 2010; Vilchez et al., 2012). However, the turnover of proteasome subunits is seldom discussed. With few exceptions, the biological significance of extensively reported proteasome phosphorylation events has been largely unknown (Kikuchi et al., 2010; Lu et al., 2008). In the present study, we have shown that PSMA7 is phosphorylated at Y106 in addition to Y153 by c-Abl kinase. Phosphorylation at both sites probably contributed to the c-Abl-mediated proteasome inhibition, whereas Y106 is the major site regulating the ubiquitin-proteasomal degradation of proteasome-unincorporated PSMA7. According to crystal structure, neither Y153 nor Y106 of PSMA7 is located on the outer surface of proteasome (Huber et al., 2012). Therefore, PSMA7 would be less phosphorylated at these sites when incorporated into the proteasome. Moreover, it should not be excluded that there are other potential phosphosites on PSMA7 or other proteasome subunits, because c-Abl could directly phosphorylate 26S proteasome in vitro (Liu et al., 2006). In eukaryotes, the absence of any 20S proteasome subunit, with the exception of pre9/α3 in *S. cerevisiae* (Velichutina et al., 2004), results in a

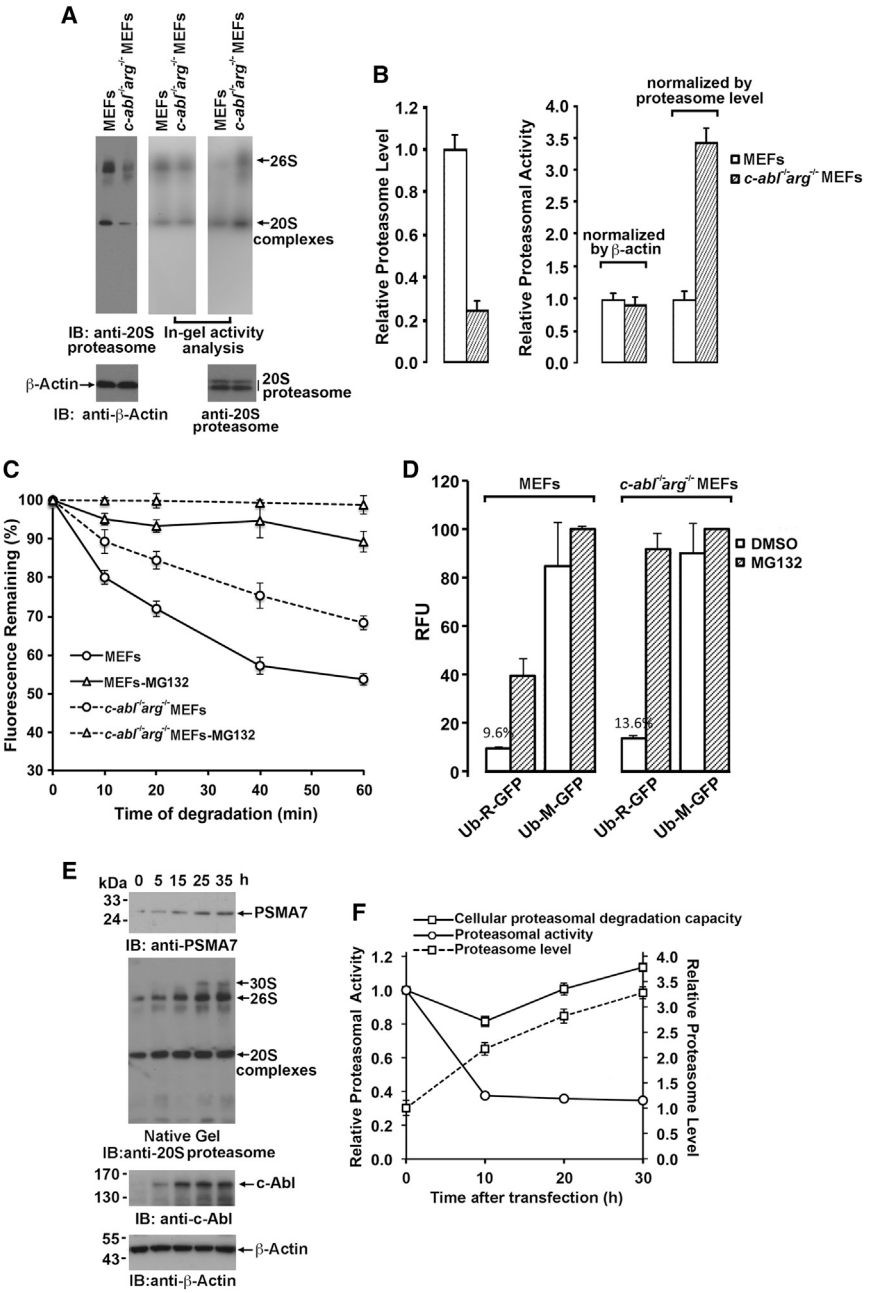

Figure 6. Dual Roles of the c-Abl Kinase in Proteasome-Dependent Proteolysis

(A and B) Extracts of the wild-type or *abl*$^{-/-}$*arg*$^{-/-}$ MEFs were subjected to native gel electrophoresis for proteasome complex resolution or SDS-PAGE and then analyzed by immunoblotting (A, left) or in-gel proteasomal peptidase activity analysis using LLVY-AMC fluorescence substrates (A, middle and right). The extracts were normalized by cellular β-actin or proteasome level as indicated. The qualification of proteasome level and activity were expressed as the mean ± SD of three independent measures (B).

(C) After CHX treatment, the fluorescence intensity of indicated cells expressing UB-R-GPF treated with or without 10 μM MG132 was chased by PE EnVision Spectrometer (Ex/Em: 485/535 nm) at indicated time points. The results were expressed as the mean ± SD of three independent measures.

(D) With (hatched bar) or without (open bar) 10 μM MG132 treatment, the fluorescence intensity of indicated cells transfected with UB-R-GPF or Ub-M-GFP was assayed as in (C). RFU, relative fluorescence units.

(E and F) *c-abl*$^{-/-}$*arg*$^{-/-}$ MEFs were electrotransfected (~70% efficiency) with a c-Abl-expressing plasmid or a control vector for indicated times. Extracts of transfected cells were subjected to immunoblotting after resolution by native gel or SDS-PAGE electrophoresis (E) and proteasomal activity assay using LLVY-AMC fluorescence substrate (F). The proteasome levels were assessed by densitometry of the western blot. Relative overall proteasomal degradation capacity (peptidase activity normalized by β-actin level; solid-line with □), relative proteasomal activity (peptidase activity normalized by cellular proteasome level; solid-line with ○), and relative 20S proteasome abundance (dashed line with □) of c-Abl-rescued *c-abl*$^{-/-}$*arg*$^{-/-}$ MEFs over control transfection were shown for each time point. The values at 0 hr were defined as 1. The results were expressed as the accessible mean ± SD of three independent experiments.

failure in 20S proteasome assembly and cell lethality (Wójcik and DeMartino, 2002). We also observed a downregulation of all 20S subunits, impaired proteasomal activity, and moderately effected viability by PSMA7 knockdown (Figures S5A and S5B), which is accordant with the finding that PSMA7 supply shortage caused by c-Abl/Arg knockout or inhibition impairs the proteasome assembly (Figure 5).

It is also intriguing that the c-Abl kinase plays dual roles in proteasome-dependent proteolysis. The depletion of *c-abl/arg* results in a significantly decreased proteasome level but an increased proteasomal activity (normalized by cellular proteasome level), which may contribute to the modest decrease of overall proteasomal degradation capacity (normalized by cellular β-actin level) of *c-abl/arg*-deficient cells (Figures 6A–6D). Although the less-efficient degradation activity is adequate for the survival of *c-abl/arg*-deficient cells, it may not be sufficient to dispose massively produced ubiquitin conjugates under cellular stresses such as heat shock, oxidative stress, starvation, or proteasome inhibition (Seifert et al., 2010; Figures 7G and S7B). According to the time-course-dependent effect of c-Abl on proteasome (Figures 6E and 6F), ROS-activated c-Abl kinase may rapidly phosphorylate and inhibit proteasome at the very early stage of oxidative stress, protecting some short-living proteins, such as p53 or p21, from proteasomal degradation and inducing cell-cycle arrest for self-restoration. At meantime, the cellular proteasome abundance is gradually increased along with Abl kinase keeping activation, contributing to the removal of accumulated

oxidatively damaged proteins and avoiding potentially toxic effects. Lowered efficiency and dynamic regulation of proteasome in *c-abl/arg*-null cells may contribute to the heightened sensitivity to ROS-induced cell apoptosis (Cao et al., 2003). c-Abl-mediated dynamic regulation of cellular proteasomal degradation activity is likely to be a significant modulator by fine-tuning protein turnover in response to stress or other environmental factors and provides insight into the mechanism of c-Abl-involved tumorigenesis and neurodegenerative diseases.

Proteasomal system is an important therapeutic target in malignant diseases treatment. Recent findings have demonstrated that knockdown of any of the 20S core subunits sensitized the cell to proteasomal inhibitor bortezomib and exhibited a synergistic lethal phenotype (Chen et al., 2010). Similarly, enhanced cell killing was observed after treatment with the proteasome inhibitor YU101 combined with knockdown of the transcription factor Nrf1 (Radhakrishnan et al., 2010). Our findings also demonstrated that the proteasomal activity in *c-abl*$^{-/-}$*arg*$^{-/-}$ MEFs with lowered proteasome abundance was more suppressed by MG132 compared to wild-type MEFs (Figure 6D), indicating that the proteasome inhibitor sensitivity may be increased by c-Abl kinase inhibition. Myeloid leukemia cells constitutively expressing Bcr-Abl have higher proteasome levels compared to normal peripheral blood cells (Kumatori et al., 1990; Magill et al., 2004). Recent studies have demonstrated that a greater than 85% decrease in K562 CML cell proliferation by combination STI571/bortezomib treatment has been observed compared to ~50% by bortezomib alone or ~10% by STI571 alone at the same concentration (Yusuf et al., 2009). Leukemic cells or mice with CML treated with STI571 or dasatinib (a second-generation Abl kinase inhibitor) combined with bortezomib exhibited suppressed tumor growth and significantly prolonged life spans, offering a potential therapeutic option for CML (Heaney et al., 2010; Hu et al., 2009). These studies strongly indicate that Abl kinase antagonists could be particularly efficacious in combination anticancer therapies with proteasome inhibitors based on their effects on Abl signaling, PSMA7, and proteasome regulation.

EXPERIMENTAL PROCEDURES

Cell Culture and Transfection

The HEK293 cells, MCF-7 cells, and MEFs derived from wild-type, *c-abl*$^{-/-}$, or *c-abl*$^{-/-}$*arg*$^{-/-}$ littermates (kindly provided by Dr. Anthony J. Koleske) were grown in DMEM (GIBCO) supplemented with 10% heat-inactivated fetal bovine serum (Hyclone), 2 mM L-glutamine, 100 units/ml penicillin, and 100 μg/ml streptomycin. K562 and HL60 cells were grown in RPMI 1640 medium (GIBCO). Cells were treated with STI571 (Novartis), MG132 (BIOMOL), lactacystin (BIOMOL), or concanamycin A (Sigma) as noted in the text. Cells were transfected with Lipofectamine 2000 or the Neon electrotransfection system (Invitrogen).

DNA Constructs

FLAG-tagged and hemagglutinin (HA)-tagged protein gene was cloned into the pcDNA3 vector (Invitrogen). Myc-tagged protein gene was cloned into the pCMV-Myc vector (Clontech). siRNAs (Table S2) were constructed into the si-STRIKE U6 Hairpin Cloning System (Promega).

Immunoprecipitation and Immunoblotting Analysis

Cell lysates were prepared in lysis buffer containing 1% Nonidet P-40 (Cao et al., 2003). Soluble proteins were subjected to immunoprecipitation with anti-FLAG (M2; Sigma F2426), anti-PSMA7 (BIOMOL PW9140 or PW8120) antibodies, or mouse immunoglobulin G (IgG) (Sigma A0910). An aliquot of the total lysate (5%; v/v) was included as a control. The immunoblotting analysis was performed with anti-PTyr (4G10; Millipore 16-105), anti-c-Abl (Santa Cruz SC-131), anti-Myc (Santa Cruz SC-40), anti-FLAG horseradish peroxidase (Sigma A8592), anti-β-actin (Santa Cruz SC-1616), anti-ubiquitin (Santa Cruz SC-8017), anti-HA (Sigma H9658), anti-BRCA1 (Santa Cruz SC-6954), or anti-20S proteasome (BIOMOL PW8195) antibodies. The antigen-antibody complexes were visualized by enhanced chemiluminescence (ECL) (GE Healthcare). Densitometry of the bands was analyzed by ImageJ (NIH). Average of three independent experiments with SDs (error bars) and p values as determined by t test were indicated.

LC-MS/MS Analysis

FLAG-tagged PSMA7 immunoprecipitates prepared from whole-cell lysates or gel-filtrated fractions were resolved by SDS-PAGE, and protein bands were excised. After adequate trypsinization, phosphopeptides were enriched with TiO_2 resin (Calbiochem). LC-electrospray ionization-MS/MS-resolved peptides were analyzed using a Q-TOF2 system (Micromass), and the data were compared against SWISSPROT using the Mascot search engine (http://www.matrixscience.com) for phosphorylation.

Gel Filtration Chromatography

Cells were lysed by one pass through a French press in lysis buffer containing 50 mM Tris-HCl (pH 7.5), 150 mM NaCl, 5 mM MgCl2, 10% glycerol (v/v), 1 mM DTT, and 2 mM ATP. After cleared by centrifugation, cell lysates were loaded on the Superdex200 gel column (HR30; GE Healthcare) and eluted with elution buffer containing 25 mM Tris-HCl (pH 7.5), 150 mM NaCl, 10% glycerol (v/v), 5 mM $MgCl_2$, and 2 mM ATP. Eluates were continuously collected by FC900 fraction collector with 1.5 ml in each fraction when 0.01 absorbance units UV absorbance was monitored. The first fraction with UV absorbance was designated as fraction no. 1. Fractions no. 4–no. 6 with peptidase activity were combined as proteasome-incorporated subunit fraction, and fractions no. 12–no. 14 were combined as proteasome-unincorporated subunit fraction (Figures S1B and S2A).

Pulse-Chase Assay

Eighteen hours after the transfection of HEK293 cells with FLAG-tagged wild-type or mutant PSMA7, cells were pulsed with [^{35}S]-methionine (NEG 709A; PerkinElmer Life and Analytical Sciences) for 1 hr in methionine-free DMEM (Invitrogen) at a concentration of 10 μCi/ml. The cells were then washed, cultured in complete DMEM supplemented with 5 mM cold methionine, and harvested at the indicated times. Anti-FLAG immunoprecipitates were subjected to SDS-PAGE and autoradiography.

In Vitro Degradation Assay

[^{35}S]-labeled PSMA7 proteins prepared by TNT Quick Coupled Transcription/Translation Systems (Promega) were purified by anti-FLAG antibody affinity chromatography. The purified proteins were preincubated with or without recombinant c-Abl kinase (Upstate Biotechnology) in kinase buffer at 37°C for 60 min and were then added to the extracts of *c-abl*$^{-/-}$*arg*$^{-/-}$ MEFs pretreated with or without the proteasome inhibitor MG132. Then, 13% trichloroacetic acid was used to sediment the undegradated [^{35}S]-labeled PSMA7 proteins and the supernatant was subjected to liquid scintillation counting for quantitation. The average counts per minute values obtained from three independent experiments were presented.

In Vitro Ubiquitination

To reconstitute the ubiquitination system in vitro, HA-BRCA1, HA-BARD, and the indicated mutants were purified from HEK293 cells using affinity chromatography with an anti-HA antibody and eluted with 10 μg/ml HA peptide (Sigma). Similarly purified FLAG-PSMA7 was incubated with either HA-BRCA1 or the I26A mutant together with or without HA-BARD at 37°C for 90 min in a buffer containing E1, UbcH5c, biotinylated ubiquitin, and ATP (Sigma). The reaction products were resolved by SDS-PAGE and were detected by immunoblotting.

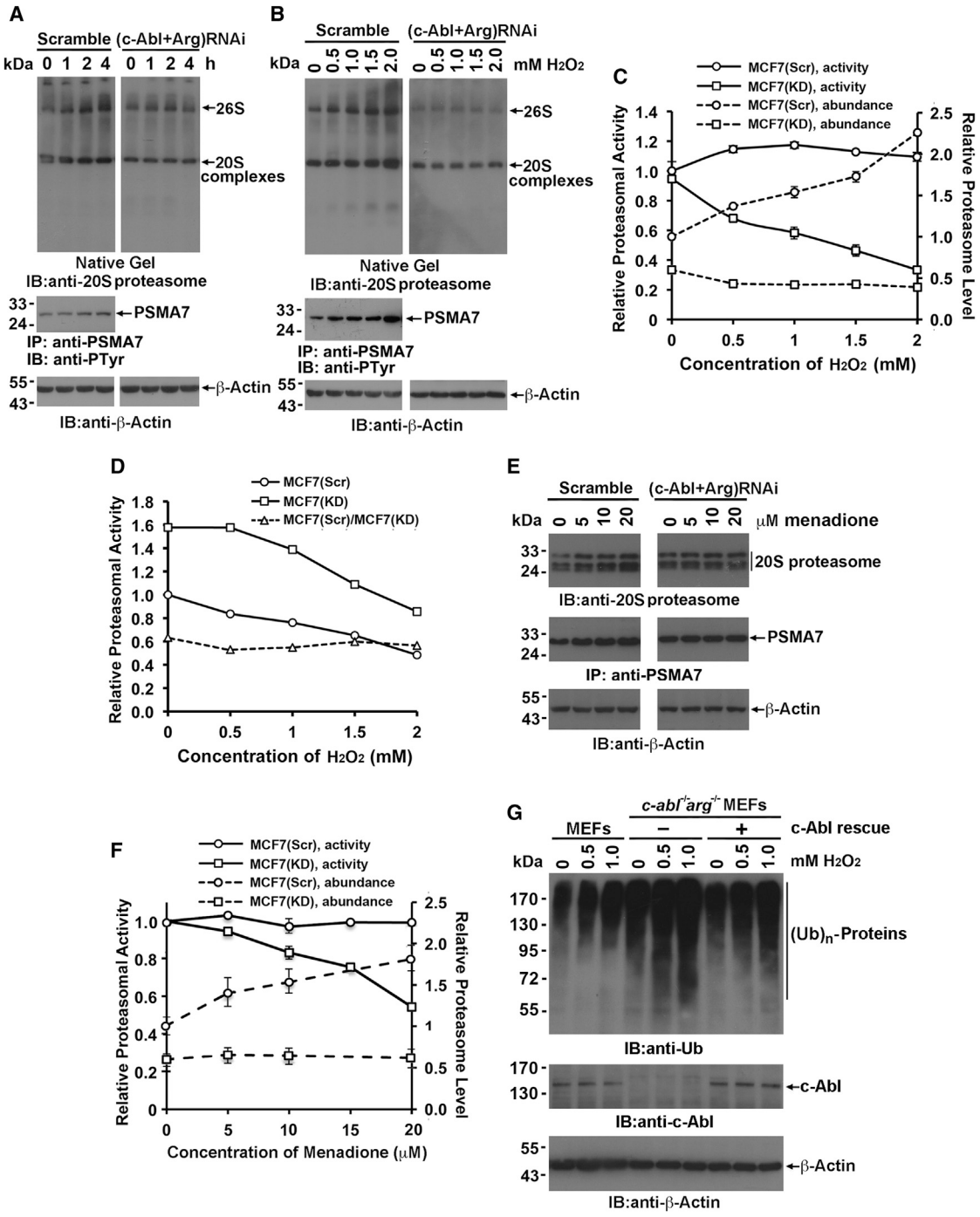

Figure 7. The Regulation of Proteasomal Activity by c-Abl Kinase in Response to ROS Stimuli

(A and B) MCF-7(Scr) or MCF-7(KD) cells were treated with 0.5 mM H_2O_2 for 0–4 hr (A) or with 0–2.0 mM H_2O_2 for 2 hr (B). Lysates or anti-PSMA7 immunoprecipitates prepared from H_2O_2-treated cells were subjected to immunoblotting after resolution by native gel or SDS-PAGE electrophoresis.

(C and D) Cell extracts described in (B) were subjected to proteasomal activity assay using LLVY-AMC fluorescence substrate. Relative overall proteasomal degradation capacity (peptidase activity normalized by β-actin level; solid-line) and relative proteasome abundance (dashed line) of indicated cells at different treatment concentrations were shown in (C). The relative proteasomal activity of indicated cells (peptidase activity normalized by cellular proteasome level; solid line) and the proteasomal activity ratio of MCF-7(Scr) and MCF-7(KD) (dashed line) at different concentrations were shown in (D). The values at 0 mM H_2O_2 treatment were defined as 1. The results in (C) were expressed as the accessible mean ± SD of three independent experiments.

(legend continued on next page)

Proteasome Peptidase Activity Assay

Cell extracts were incubated in peptidase reaction buffer containing 0.1 mM AMC-conjugated peptide substrates (Succinyl-LLVY-AMC; BIOMOL), 20 mM Tris-HCl (pH 7.4), 0.5 mM EDTA, 5 mM $MgCl_2$, 1 mM DTT, 2 mM ATP, and 0.02% SDS for 30 min at 37°C. Fluorescence was assayed by fluorescence spectrometer (Ex/Em: 380/460 nm; Fluoroskan Ascent FL; Thermo Scientific). The relative fluorescence intensity was calculated from the mean ± SD of three independent experiments.

Native-PAGE Resolution of Proteasome Complexes

Cells were lysed by one pass through a French press in lysis buffer as described above. The 2× native loading buffer contains 250 mM Tris-HCl (pH 7.5), 50% glycerol (v/v), and 0.007% xylene cyanol (w/v). After resolved by NuPAGE 3%–8% Tris-Acetate Gel (Invitrogen), the proteins from the native gel were transferred to polyvinylidene fluoride membrane for immunoblotting detection. The commercially purified 26S (PW9310; BIOMOL) and 20S (PW8720; BIOMOL) proteasomes were used as a size marker for the native gel (Figure S1B, left).

For in-gel proteasomal activity assay, incubate the native gel in proteasome peptidase reaction buffer containing Succinyl-LLVY-AMC as described above for 20 min at 37°C. For stimulation of the 20S peptidase activity, add 0.02% SDS. Then, visualize the gel on a UV transilluminator with a wavelength of 365 nm.

The Proteasomal Activity Assay in Living Cells

The detail of proteasomal activity assay in living cells has been described previously (Dantuma et al., 2000). The wild-type or *c-abl*$^{-/-}$*arg*$^{-/-}$ MEFs were transfected with UB-R-GFP- or UB-M-GFP-expressing plasmid for 24 hr. After treated with or without 10 μM MG132 for 10 hr, the cells were detached from the culture dish by trypsin digesting, washed, and resuspended by 1× PBS buffer and transferred into 96-well plate. The fluorescence intensity of each well was assayed by PE EnVision Spectrometer (Ex/Em: 485/535 nm). The relative fluorescence intensity was calculated from the mean ± SD of three independent experiments.

Animal Experiment

The BALB/c mice were orally administrated with 50 mg/kg of STI571 or saline for 2 weeks. The proteasome levels in hepatic tissue of mice were analyzed by immunoblotting. Animal studies were approved by Institutional Ethics Committee.

SUPPLEMENTAL INFORMATION

Supplemental Information includes seven figures and two tables and can be found with this article online at http://dx.doi.org/10.1016/j.celrep.2014.12.044.

AUTHOR CONTRIBUTIONS

D.L., Q.D., Q.T., J.G., Y.C., X.J., R.X., and X.L. performed the experiments. Q.M. and C.C. designed and supervised the research. J.Y. and W.L. analyzed data. Y.J. and P.L. developed protocols and provided reagents. X.L. and C.C. wrote the paper. D.T.W. revised the manuscript.

ACKNOWLEDGMENTS

This investigation was supported by grant 2012CB518900 awarded by the National "973" program of China and grants 30670407 and 30871240 awarded by the Natural Science Foundation of China. The authors acknowledge Dr. Tony Koleske for the *c-abl*$^{-/-}$ and *c-abl*$^{-/-}$*arg*$^{-/-}$ MEFs.

Received: August 12, 2014
Revised: November 3, 2014
Accepted: December 5, 2014
Published: January 22, 2015

REFERENCES

Aiken, C.T., Kaake, R.M., Wang, X., and Huang, L. (2011). Oxidative stress-mediated regulation of proteasome complexes. Mol. Cell. Proteomics *10*, 006924.

Bedford, L., Paine, S., Sheppard, P.W., Mayer, R.J., and Roelofs, J. (2010). Assembly, structure, and function of the 26S proteasome. Trends Cell Biol. *20*, 391–401.

Cao, C., Leng, Y., and Kufe, D. (2003). Catalase activity is regulated by c-Abl and Arg in the oxidative stress response. J. Biol. Chem. *278*, 29667–29675.

Chen, S., Blank, J.L., Peters, T., Liu, X.J., Rappoli, D.M., Pickard, M.D., Menon, S., Yu, J., Driscoll, D.L., Lingaraj, T., et al. (2010). Genome-wide siRNA screen for modulators of cell death induced by proteasome inhibitor bortezomib. Cancer Res. *70*, 4318–4326.

Cho, S., Choi, Y.J., Kim, J.M., Jeong, S.T., Kim, J.H., Kim, S.H., and Ryu, S.E. (2001). Binding and regulation of HIF-1alpha by a subunit of the proteasome complex, PSMA7. FEBS Lett. *498*, 62–66.

Dächsel, J.C., Lücking, C.B., Deeg, S., Schultz, E., Lalowski, M., Casademunt, E., Corti, O., Hampe, C., Patenge, N., Vaupel, K., et al. (2005). Parkin interacts with the proteasome subunit alpha4. FEBS Lett. *579*, 3913–3919.

Dantuma, N.P., Lindsten, K., Glas, R., Jellne, M., and Masucci, M.G. (2000). Short-lived green fluorescent proteins for quantifying ubiquitin/proteasome-dependent proteolysis in living cells. Nat. Biotechnol. *18*, 538–543.

Ding, Q., Reinacker, K., Dimayuga, E., Nukala, V., Drake, J., Butterfield, D.A., Dunn, J.C., Martin, S., Bruce-Keller, A.J., and Keller, J.N. (2003). Role of the proteasome in protein oxidation and neural viability following low-level oxidative stress. FEBS Lett. *546*, 228–232.

Finley, D. (2009). Recognition and processing of ubiquitin-protein conjugates by the proteasome. Annu. Rev. Biochem. *78*, 477–513.

Foray, N., Marot, D., Randrianarison, V., Venezia, N.D., Picard, D., Perricaudet, M., Favaudon, V., and Jeggo, P. (2002). Constitutive association of BRCA1 and c-Abl and its ATM-dependent disruption after irradiation. Mol. Cell. Biol. *22*, 4020–4032.

Groll, M., Ditzel, L., Löwe, J., Stock, D., Bochtler, M., Bartunik, H.D., and Huber, R. (1997). Structure of 20S proteasome from yeast at 2.4 A resolution. Nature *386*, 463–471.

Grune, T., Catalgol, B., Licht, A., Ermak, G., Pickering, A.M., Ngo, J.K., and Davies, K.J. (2011). HSP70 mediates dissociation and reassociation of the 26S proteasome during adaptation to oxidative stress. Free Radic. Biol. Med. *51*, 1355–1364.

Heaney, N.B., Pellicano, F., Zhang, B., Crawford, L., Chu, S., Kazmi, S.M., Allan, E.K., Jorgensen, H.G., Irvine, A.E., Bhatia, R., and Holyoake, T.L. (2010). Bortezomib induces apoptosis in primitive chronic myeloid leukemia cells including LTC-IC and NOD/SCID repopulating cells. Blood *115*, 2241–2250.

Heink, S., Ludwig, D., Kloetzel, P.M., and Krüger, E. (2005). IFN-gamma-induced immune adaptation of the proteasome system is an accelerated and transient response. Proc. Natl. Acad. Sci. USA *102*, 9241–9246.

Hu, Z., Pan, X.F., Wu, F.Q., Ma, L.Y., Liu, D.P., Liu, Y., Feng, T.T., Meng, F.Y., Liu, X.L., Jiang, Q.L., et al. (2009). Synergy between proteasome inhibitors and imatinib mesylate in chronic myeloid leukemia. PLoS ONE *4*, e6257.

Huber, E.M., Basler, M., Schwab, R., Heinemeyer, W., Kirk, C.J., Groettrup, M., and Groll, M. (2012). Immuno- and constitutive proteasome crystal

(E and F) MCF-7(Scr) or MCF-7(KD) cells were treated with 0–20 μM menadione for 3 hr. Cells extracts were analyzed by immunoblotting (E) or subjected to proteasomal activity assay as described in (C) (F).

(G) Indicated cells were treated with or without H_2O_2 for 3 hr and then analyzed by immunoblotting. The electrotransfection efficiency of *c-abl*$^{-/-}$*arg*$^{-/-}$ MEFs for c-Abl rescue was about 70%.

structures reveal differences in substrate and inhibitor specificity. Cell *148*, 727–738.

Jørgensen, L., and Hendil, K.B. (1999). Proteasome subunit zeta, a putative ribonuclease, is also found as a free monomer. Mol. Biol. Rep. *26*, 119–123.

Kikuchi, J., Iwafune, Y., Akiyama, T., Okayama, A., Nakamura, H., Arakawa, N., Kimura, Y., and Hirano, H. (2010). Co- and post-translational modifications of the 26S proteasome in yeast. Proteomics *10*, 2769–2779.

Kim, W., Bennett, E.J., Huttlin, E.L., Guo, A., Li, J., Possemato, A., Sowa, M.E., Rad, R., Rush, J., Comb, M.J., et al. (2011). Systematic and quantitative assessment of the ubiquitin-modified proteome. Mol. Cell *44*, 325–340.

Koleske, A.J., Gifford, A.M., Scott, M.L., Nee, M., Bronson, R.T., Miczek, K.A., and Baltimore, D. (1998). Essential roles for the Abl and Arg tyrosine kinases in neurulation. Neuron *21*, 1259–1272.

Kumatori, A., Tanaka, K., Inamura, N., Sone, S., Ogura, T., Matsumoto, T., Tachikawa, T., Shin, S., and Ichihara, A. (1990). Abnormally high expression of proteasomes in human leukemic cells. Proc. Natl. Acad. Sci. USA *87*, 7071–7075.

Le Tallec, B., Barrault, M.B., Courbeyrette, R., Guérois, R., Marsolier-Kergoat, M.C., and Peyroche, A. (2007). 20S proteasome assembly is orchestrated by two distinct pairs of chaperones in yeast and in mammals. Mol. Cell *27*, 660–674.

Lee, B.H., Lee, M.J., Park, S., Oh, D.C., Elsasser, S., Chen, P.C., Gartner, C., Dimova, N., Hanna, J., Gygi, S.P., et al. (2010). Enhancement of proteasome activity by a small-molecule inhibitor of USP14. Nature *467*, 179–184.

Leggett, D.S., Hanna, J., Borodovsky, A., Crosas, B., Schmidt, M., Baker, R.T., Walz, T., Ploegh, H., and Finley, D. (2002). Multiple associated proteins regulate proteasome structure and function. Mol. Cell *10*, 495–507.

Lehmann, A., Niewienda, A., Jechow, K., Janek, K., and Enenkel, C. (2010). Ecm29 fulfils quality control functions in proteasome assembly. Mol. Cell *38*, 879–888.

Li, X., Ma, Q., Wang, J., Liu, X., Yang, Y., Zhao, H., Wang, Y., Jin, Y., Zeng, J., Li, J., et al. (2010). c-Abl and Arg tyrosine kinases regulate lysosomal degradation of the oncoprotein Galectin-3. Cell Death Differ. *17*, 1277–1287.

Liu, X., Huang, W., Li, C., Li, P., Yuan, J., Li, X., Qiu, X.B., Ma, Q., and Cao, C. (2006). Interaction between c-Abl and Arg tyrosine kinases and proteasome subunit PSMA7 regulates proteasome degradation. Mol. Cell *22*, 317–327.

Lu, H., Zong, C., Wang, Y., Young, G.W., Deng, N., Souda, P., Li, X., Whitelegge, J., Drews, O., Yang, P.Y., and Ping, P. (2008). Revealing the dynamics of the 20 S proteasome phosphoproteome: a combined CID and electron transfer dissociation approach. Mol. Cell. Proteomics *7*, 2073–2089.

Magill, L., Lynas, J., Morris, T.C., Walker, B., and Irvine, A.E. (2004). Proteasome proteolytic activity in hematopoietic cells from patients with chronic myeloid leukemia and multiple myeloma. Haematologica *89*, 1428–1433.

Murata, S., Yashiroda, H., and Tanaka, K. (2009). Molecular mechanisms of proteasome assembly. Nat. Rev. Mol. Cell Biol. *10*, 104–115.

Navon, A., and Goldberg, A.L. (2001). Proteins are unfolded on the surface of the ATPase ring before transport into the proteasome. Mol. Cell *8*, 1339–1349.

Pendergast, A.M. (2002). The Abl family kinases: mechanisms of regulation and signaling. Adv. Cancer Res. *85*, 51–100.

Pickart, C.M., and Cohen, R.E. (2004). Proteasomes and their kin: proteases in the machine age. Nat. Rev. Mol. Cell Biol. *5*, 177–187.

Pickering, A.M., Linder, R.A., Zhang, H., Forman, H.J., and Davies, K.J. (2012). Nrf2-dependent induction of proteasome and Pa28$\alpha\beta$ regulator are required for adaptation to oxidative stress. J. Biol. Chem. *287*, 10021–10031.

Plattner, R., Kadlec, L., DeMali, K.A., Kazlauskas, A., and Pendergast, A.M. (1999). c-Abl is activated by growth factors and Src family kinases and has a role in the cellular response to PDGF. Genes Dev. *13*, 2400–2411.

Radhakrishnan, S.K., Lee, C.S., Young, P., Beskow, A., Chan, J.Y., and Deshaies, R.J. (2010). Transcription factor Nrf1 mediates the proteasome recovery pathway after proteasome inhibition in mammalian cells. Mol. Cell *38*, 17–28.

Reinheckel, T., Sitte, N., Ullrich, O., Kuckelkorn, U., Davies, K.J., and Grune, T. (1998). Comparative resistance of the 20S and 26S proteasome to oxidative stress. Biochem. J. *335*, 637–642.

Ren, R., Mayer, B.J., Cicchetti, P., and Baltimore, D. (1993). Identification of a ten-amino acid proline-rich SH3 binding site. Science *259*, 1157–1161.

Rush, J., Moritz, A., Lee, K.A., Guo, A., Goss, V.L., Spek, E.J., Zhang, H., Zha, X.M., Polakiewicz, R.D., and Comb, M.J. (2005). Immunoaffinity profiling of tyrosine phosphorylation in cancer cells. Nat. Biotechnol. *23*, 94–101.

Seifert, U., Bialy, L.P., Ebstein, F., Bech-Otschir, D., Voigt, A., Schröter, F., Prozorovski, T., Lange, N., Steffen, J., Rieger, M., et al. (2010). Immunoproteasomes preserve protein homeostasis upon interferon-induced oxidative stress. Cell *142*, 613–624.

Sun, X., Majumder, P., Shioya, H., Wu, F., Kumar, S., Weichselbaum, R., Kharbanda, S., and Kufe, D. (2000). Activation of the cytoplasmic c-Abl tyrosine kinase by reactive oxygen species. J. Biol. Chem. *275*, 17237–17240.

Sy, S.M., Huen, M.S., and Chen, J. (2009). PALB2 is an integral component of the BRCA complex required for homologous recombination repair. Proc. Natl. Acad. Sci. USA *106*, 7155–7160.

Velichutina, I., Connerly, P.L., Arendt, C.S., Li, X., and Hochstrasser, M. (2004). Plasticity in eucaryotic 20S proteasome ring assembly revealed by a subunit deletion in yeast. EMBO J. *23*, 500–510.

Vilchez, D., Boyer, L., Morantte, I., Lutz, M., Merkwirth, C., Joyce, D., Spencer, B., Page, L., Masliah, E., Berggren, W.T., et al. (2012). Increased proteasome activity in human embryonic stem cells is regulated by PSMD11. Nature *489*, 304–308.

Wójcik, C., and DeMartino, G.N. (2002). Analysis of Drosophila 26 S proteasome using RNA interference. J. Biol. Chem. *277*, 6188–6197.

Xie, Y., and Varshavsky, A. (2001). RPN4 is a ligand, substrate, and transcriptional regulator of the 26S proteasome: a negative feedback circuit. Proc. Natl. Acad. Sci. USA *98*, 3056–3061.

Yusuf, B., Oztekin, C., and Yonca, B. (2009). Inhibition of proteasome by bortezomib increase chemosensitivity of bcr/abl positive human k562 chronic myleoid leukemia cells to imatinib. Health *1*, 320–324.